Limnol. Oceanogr., 51(1), 2006, 166–176

Climate effect on food supply to depths greater than 4,000 meters in the northeast Pacific

K. L. Smith, Jr.,[1] R. J. Baldwin, and H. A. Ruhl
Marine Biology Research Division, Scripps Institution of Oceanography, University of California, San Diego, 9500 Gilman Drive, La Jolla, California 92093-0202

M. Kahru and B. G. Mitchell
Integrative Oceanography Division, Scripps Institution of Oceanography, University of California, San Diego, 9500 Gilman Drive, La Jolla, California 92093-0218

R. S. Kaufmann
Marine Science and Environmental Studies Department, University of San Diego, 5998 Alcalá Park, San Diego, California 92110

Abstract

A long time-series study was conducted over 15 yr (1989–2004) to measure particulate organic carbon (POC) flux as an estimate of food supply reaching >4,000-m depth in the northeast Pacific. Sequencing sediment traps were moored at 3,500-and 4,050-m depth, 600 and 50 m above the seafloor, respectively, to collect sinking particulate matter with 10-d resolution. POC fluxes were compared with three climate indices in the Pacific: the basin-scale multivariate El Niño Southern Oscillation index (MEI) and northern oscillation index (NOI) and the regional-scale Bakun upwelling index (BUI). The NOI and MEI correlated significantly with POC flux, lagged earlier by 6–10 months, respectively. The BUI also correlated with POC flux, lagged by 2–3 months, suggesting a direct relationship between upwelling intensity and rates of POC supply to abyssal depths. Satellite ocean color data for the surface above the study site were used to estimate chlorophyll *a* concentrations and, combined with sea surface temperature and photosynthetically available radiation, to estimate net primary production and export flux (EF) from the euphotic zone. EF was significantly correlated with POC flux, lagged earlier by 0–3 months. An empirical model to estimate POC flux, with the use of NOI, BUI, and EF, yielded significant agreement with measured fluxes. Modeling of deep-sea processes on broad spatial and temporal scales with climate indices and satellite sensing now appears feasible.

Early impressions of a vast deep ocean supplied with a constant rain of small organic particles from surface waters slowly have given way to the reality of a far more dynamic environment experiencing fluctuations in food supply on timescales of days to years. Temporal variation in the supply of food from the pelagic realm has been linked to changes in deep-sea benthic community processes (e.g., Smith and Kaufmann 1999); however, little is known about the influence of climate on the deep-sea floor, which covers almost two thirds of our planet. Climate change has been correlated with planktonic community dynamics in surface waters of the ocean (Roemmich and McGowan 1995; Kahru and Mitchell 2002; McGowan et al. 2003). Because the primary food supply for the deep sea originates in surface waters, it has been hypothesized that temporal changes in planktonic communities will affect biological processes in the deep ocean (Eppley and Peterson 1979; Deuser and Ross 1980; Smith and Kaufmann 1999). Although temporal changes have been reported, both for fluxes of particulate organic matter reaching the seafloor and seasonal shifts in the rates of benthic community processes (Smith and Baldwin 1984; Baldwin et al. 1998), the long-term studies necessary to relate climate change to abyssal processes have been difficult to achieve.

Large-scale climate events, such as the El Niño Southern Oscillation (ENSO), strongly influence marine communities on global scales. Now evidence is accumulating that longer term climatic regime shifts, on the order of decades, also affect coastal and upper ocean communities (Bograd et al. 2000; Chavez et al. 2003). Interdecadal shifts in coastal benthic community structure have been reported and linked to changes in sea surface temperature (SST) associated with climate change (e.g., Sagarin et al. 1999). Given these results in shallow-water marine systems, it seems reasonable to ask whether the influence of climatically induced shifts extends to deep-sea benthic assemblages separated by >4,000 m from the air–sea interface and upper ocean phenomena.

Time-series measurements in the deep sea are rare, but

[1] Corresponding author. (ksmith@ucsd.edu).

Acknowledgments

We especially thank our colleagues Rob Glatts, Fred Uhlman, and Bob Wilson for their support throughout this study. We thank the SeaWiFS Project and the distributed active archive center (DAAC) for SeaWiFS, OCTS, and MODIS data and the Jet Propulsion Laboratory DAAC for SST data. Constructive comments were provided by the reviewers and the associate editor.

This research was supported by NSF grants OCE89-22620, OCE92-17334, OCE98-07103, and OCE0242472 to K.L.S., as well as funding from the University of California and Scripps Institution of Oceanography. Financial support to M.K. and B.G.M. was provided by NASA (NAG5-6559).

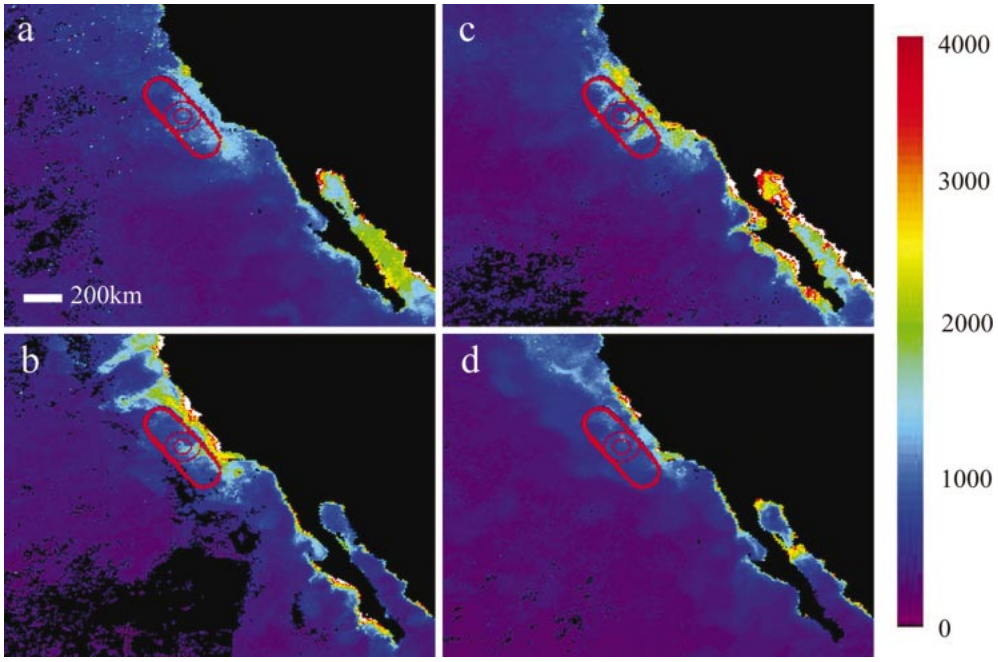

Fig. 1. Composite satellite images of net primary production (mg C m^{-2} d^{-1}) for 4 months overlaid by three spatial configurations (50- and 100-km-radius circles and 600- × 200-km oval) centered over Sta. M. (a) January 1999 with low primary production, (b) April 1999 showing elevated production in plumes extending from the California coast, (c) July 1999 with high nearshore production, and (d) October 1999 showing low production along coast.

previous results have suggested that abyssal community processes are correlated with climate-related events. A long-term discrepancy was found between the supply of food in the form of sinking particulate matter collected at abyssal depths and the energetic demand by the benthic community in the northeast Pacific Ocean from 1989 to 1996 (Smith and Kaufmann 1999; Smith et al. 2001). It was hypothesized that continuation of such long-term deficits might lead to structural changes in benthic communities. A major shift in species composition and abundance of dominant epibenthic megafauna was recorded at this same station from 1989 to 2002 and correlated with changing food supply and climate indices indicative of ENSO events (Ruhl and Smith 2004). Similarly, at an abyssal station in the northeast Atlantic, a dramatic change in species composition of dominant benthic fauna was observed over a decade, with changing food supply and climate implicated as probable causes (Billett et al. 2001).

Over the past 15 yr, we have monitored an abyssal station (Sta. M) in the northeast Pacific to study benthic community responses to food supply. We have examined the relationship between climate indices and observed changes in this deep-sea community on long timescales (more than a decade) with relatively high temporal resolution (days to months). Comparison of the estimated food supply reaching the seafloor as particulate organic carbon (POC) and the food demand by the benthic community, as estimated from sediment community oxygen consumption (SCOC), revealed a decreasing trend from POC : SCOC = 1.0 in 1989 to 0.1 in 1996 (Smith and Kaufmann 1999), followed by a sharp increase to >1.0 in 1998 (Smith et al. 2001). These observations prompted questions concerning long-term changes in sinking particulate organic material at abyssal depths and their possible connection to climate change and surface-water processes over similarly long timescales. Here, we address two questions: (1) What is the relationship between climate indices and abyssal food supply (POC flux) on long timescales? (2) What is the relationship between surface-water characteristics and abyssal food supply (POC flux) on long timescales?

Methods

The study site, Sta. M (34°50′N, 123°0′W, 4,100-m depth), is located in the California Current upwelling region, which experiences high seasonal variability in surface-water primary production. This abyssal area is characterized by low seafloor relief (<100 m over 1,600 km^2), with oxygenated silty-clay sediments and overlying water containing 146 μmol O_2 L^{-1} (Smith and Druffel 1998).

Current meter records from three altitudes above the bottom in the benthic boundary layer (BBL) showed mean current speeds of 2.3–3.6 cm s^{-1} and decreased flow rates near the seafloor (Beaulieu and Baldwin 1998). Fluxes of particulate matter entering the BBL varied seasonally, with primary peaks in early summer and secondary peaks in late fall (Baldwin et al. 1998). Detrital aggregates have been observed on the seafloor at Sta. M, typically arriving in summer and remaining visible through late fall (e.g., Smith et al. 1998). However, there have been marked deviations from this pattern, especially during climatic perturbations such as the 1992–1993 ENSO event when particulate organic matter fluxes were greatly reduced (Baldwin et al. 1998).

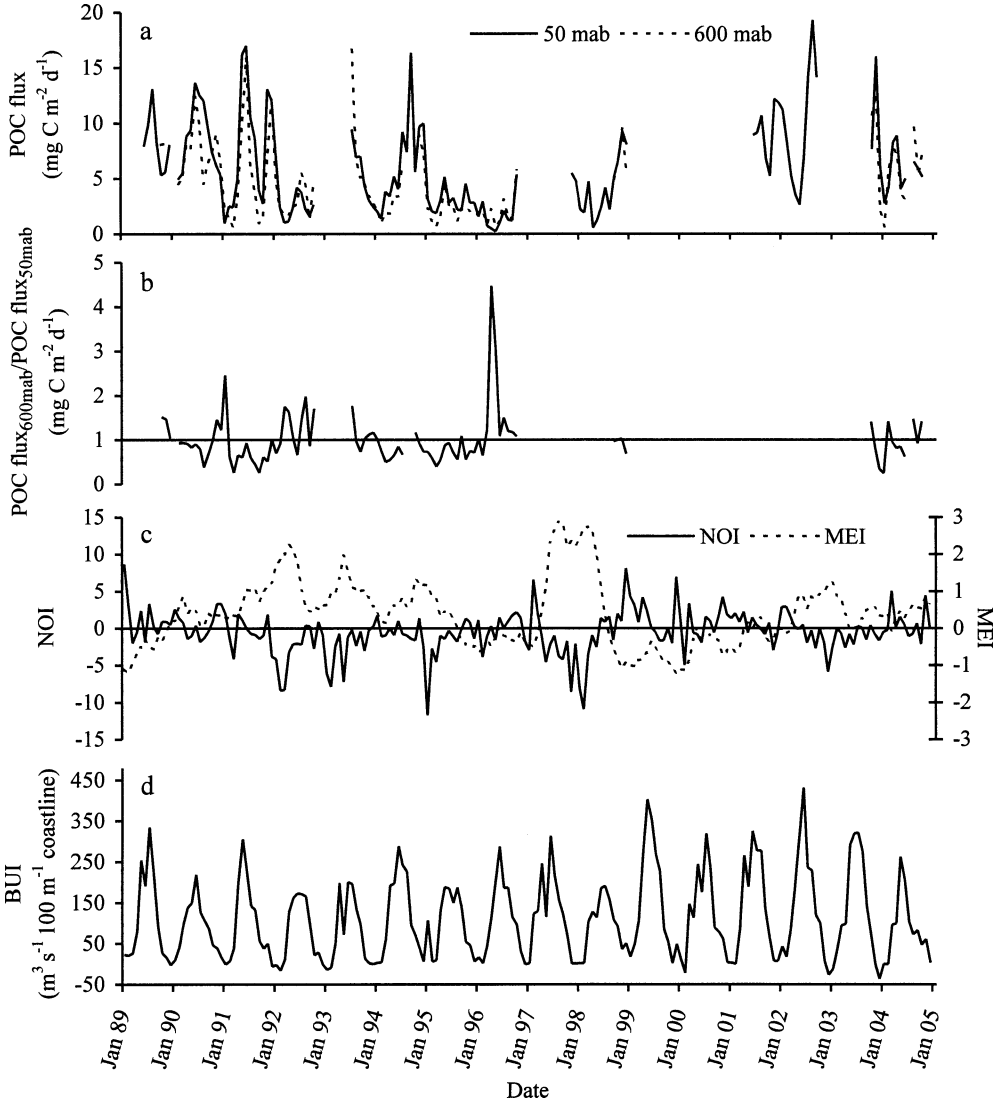

Fig. 2. Long time-series measurements of abyssal particulate organic carbon (POC) fluxes from June 1989 through October 2004 at Sta. M in the northeast Pacific compared with three climate indices. (a) POC fluxes at 50 and 600 mab (mg C m^{-2} d^{-1}). (b) The ratio of POC flux at 600 and 50 mab during periods when synchronous measurements were available. (c) northern oscillation index (NOI) and multivariate ENSO index (MEI), both computed monthly. (d) Bakun upwelling index (BUI) calculated for a 3° × 3° area centered at 36°N, 122°W.

Data from sediment traps and satellite-based sensors along with climate indices were used to examine the relationship between sea surface events and deep-ocean food supply. Sequencing conical sediment traps, each with an effective mouth opening of 0.25 m^2, were moored at 600 and 50 m above the bottom at 3,500- and 4,050-m depth, respectively (Baldwin et al. 1998). Trap sequencers were programmed with a sampling resolution of 10 d to collect sinking particulate matter in sampling cups poisoned with 3.0 mmol $HgCl_2$. In the laboratory, the collected particulate matter was analyzed in duplicate for total and inorganic carbon, with organic carbon determined by difference following methods described by Baldwin et al. (1998). Particulate organic carbon (POC) was calculated as monthly averages per square meter from the integrated 10-d fluxes.

To examine the correlation between the pelagically derived food supply (POC flux) and climate, three climate indices were chosen. The multivariate ENSO index (MEI) is computed monthly with the use of sea level pressure, surface winds, SST, surface air temperature, and cloudiness (Wolter and Timlin 1998; www.cdc.noaa.gov/people/klaus.wolter/MEI) and is positive during ENSO events as a result of weaker coastal upwelling and warmer upper ocean temperatures in the eastern Pacific. The monthly northern oscillation index (NOI) is calculated from sea level pressure anomalies in the northeast and southwest Pacific and is negative during ENSO events (Schwing et al. 2002; www.pfeg.noaa.gov/products/PFEL/modeled/indices/NOIx). A more regional indicator, the monthly Bakun upwelling index (BUI), is estimated from Ekman transport on the basis of geostrophic wind stress

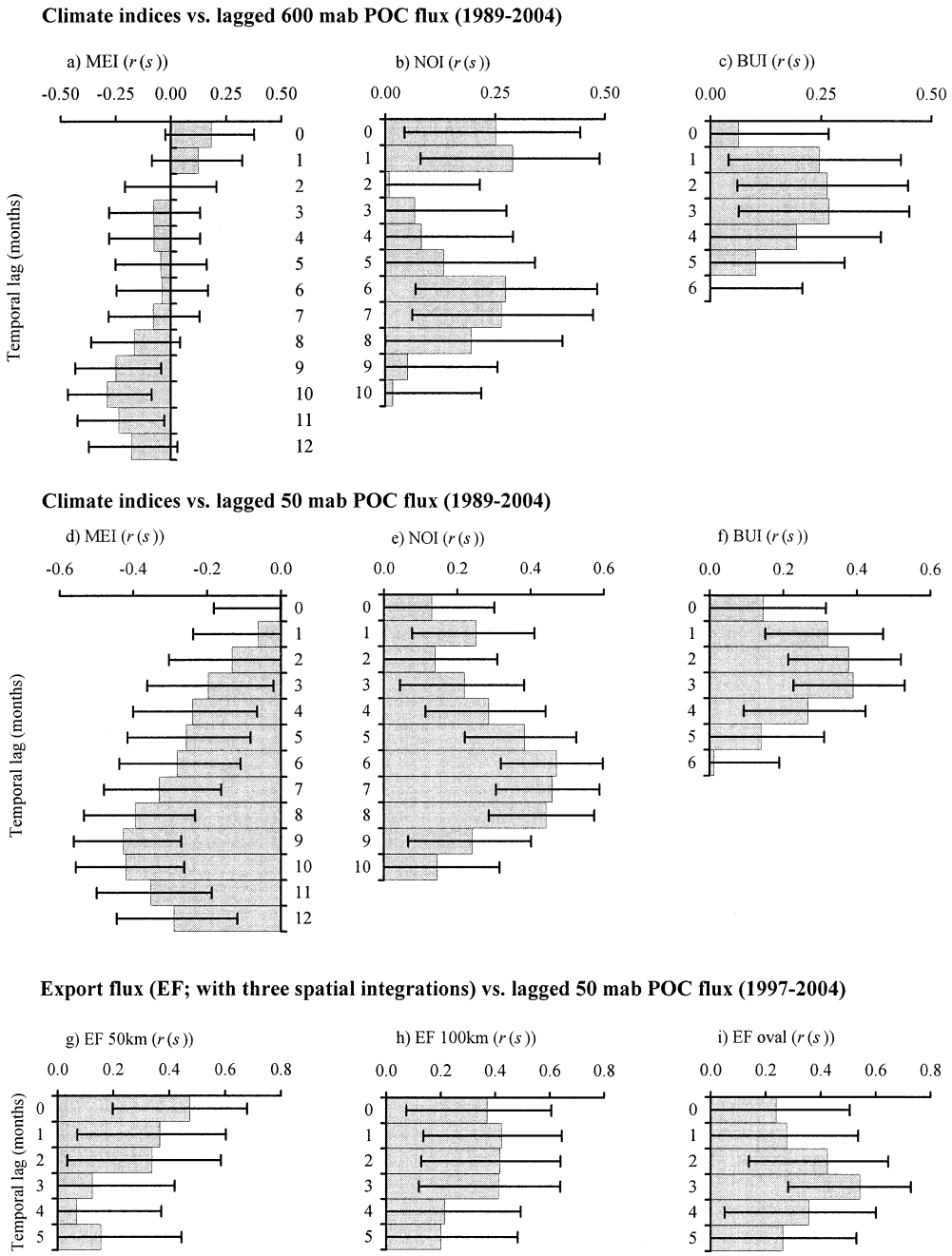

Fig. 3. Spearman rank cross-correlation analysis of monthly climate indices and export flux lagged to measured POC flux (600 and 50 mab) at Sta. M. (a) MEI lagged to $POC_{600\ mab}$ flux. (b) NOI lagged to $POC_{600\ mab}$ flux. (c) BUI lagged to $POC_{600\ mab}$ flux. (d) MEI lagged to $POC_{50\ mab}$ flux. (e) NOI lagged to $POC_{50\ mab}$ flux. (f) BUI lagged to $POC_{50\ mab}$ flux. Export flux lagged to POC $flux_{50\ mab}$ for (g) 50-km-radius circle, (h) 100-km-radius circle, and (i) 600- × 200-km oval over Sta. M. Error bars represent 95% confidence intervals for each month.

(Bakun 1973) and was calculated for a 3° by 3° coordinate area centered northeast of Sta. M at 36°N, 122°W (www.pfeg.noaa.gov/products/PFEL/modeled/indices/upwelling/upwelling). The highest values of the BUI are associated with periods of intense upwelling and lower SSTs.

Starting in November 1996, a nearly continuous time series of satellite images is available by combining data from several missions (OCTS [Ocean Color and Temperature Scanner], SeaWiFS [Sea-viewing Wide Field-of-view Sensor], Terra-MODIS [Moderate Resolution Imaging Spectroradiometer], Aqua-MODIS). An extensive ocean optics and phytoplankton pigment data set collected during California Cooperative Oceanic Fisheries Investigations (CalCOFI) cruises composed 30% of the original NASA SeaWiFS chlorophyll algorithm data set (Mitchell and Kahru 1998; O'Reilly et al. 1998), and the accuracy of chlorophyll re-

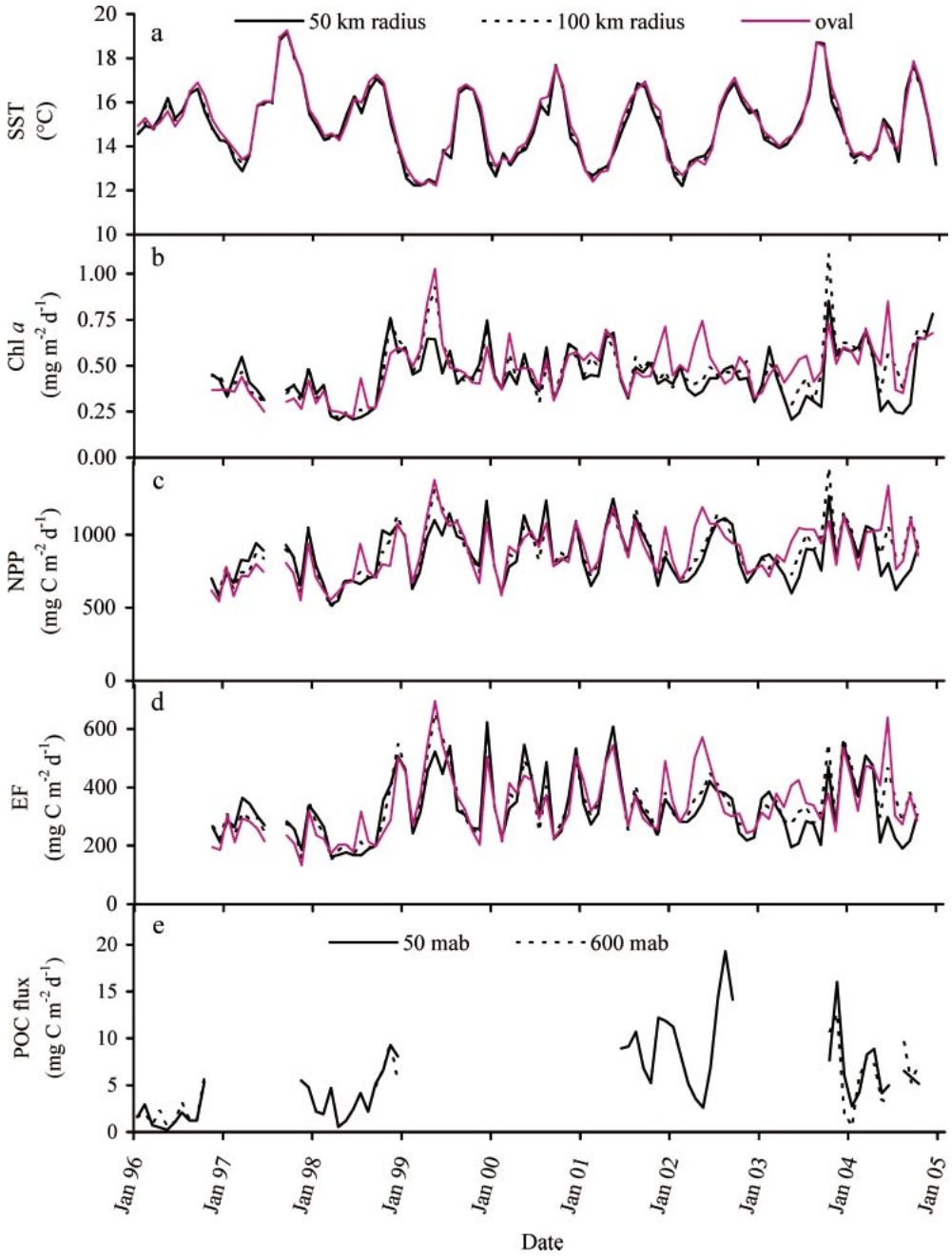

Fig. 4. Comparison of sea-surface temperature (SST), estimated surface chlorophyll *a* (Chl *a*), net primary production (NPP), and export flux (EF) from satellite data for comparison with POC flux measured at 600 and 50 mab (3,500- and 4,050-m depth) at Sta. M between January 1996 and October 2004. (a) SST derived from AVHRR (Advanced Very High Resolution Radiometer) images. (b) Chl *a* derived from satellite imaging databases (OCTS and SeaWiFS). (c) NPP computed from satellite Chl *a*, PAR, and SST with the use of the vertically generalized production model (VGPM) of Behrenfeld and Falkowski (1997). (d) Export flux (EF) from the euphotic zone computed from NPP and SST by the model of Laws (2004). (e) POC flux measured at 600 and 50 mab.

trieval for the California Current region has been summarized by Kahru and Mitchell (2001). Satellite SST data are available from the early 1980s, with accuracy better than 0.5°C. In this study, we used monthly composited satellite data. Given the hypothesized broad area of the surface ocean that contributes to sinking particulate matter reaching abyssal depths (Siegel and Deuser 1997; Siegel and Armstrong 2002), we chose sea surface areas (catchment areas) that best fit the flow field and continental influences surrounding Sta. M. SSTs and parameters depending on ocean color were calculated for three areas: 50- and 100-km-radius circles with centers at Sta. M and a 600- × 200-km oval, with the major

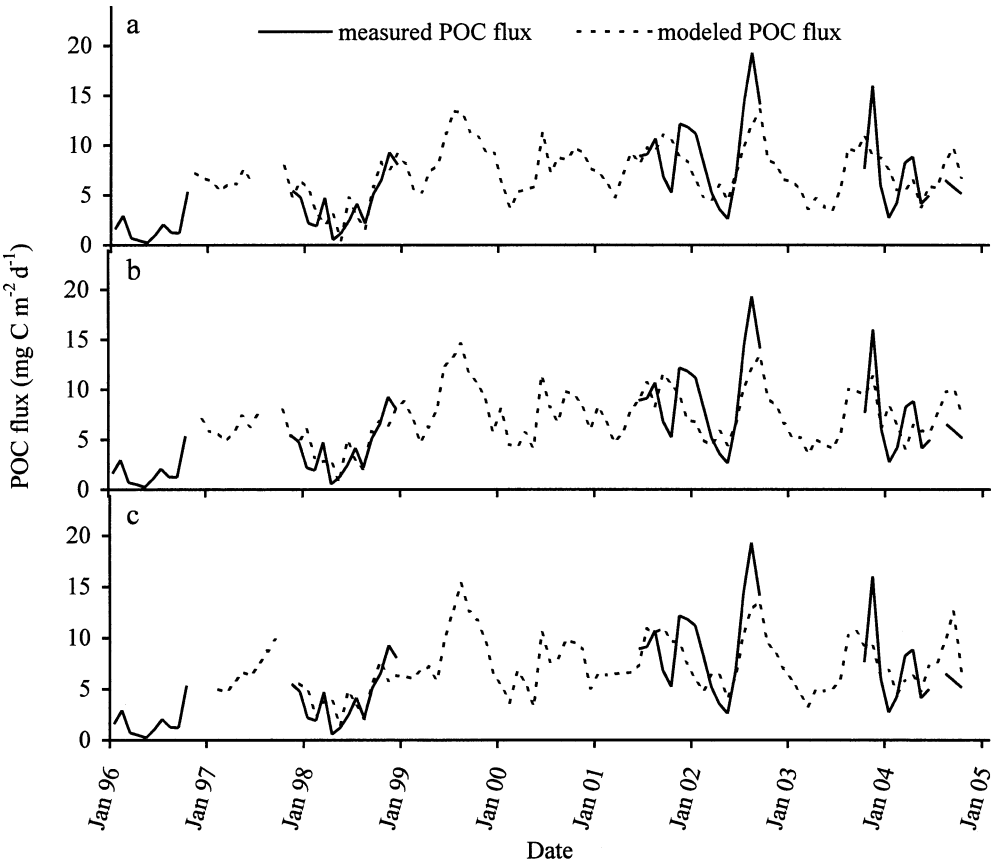

Fig. 5. Empirical model results for $POC_{50\ mab}$ flux with the use of temporally lagged BUI, NOI, and export flux (EF) over the period from November 1996 through October 2004 for each of three catchment areas centered over Sta. M compared with the measured $POC_{50\ mab}$ flux for a (a) 50-km-radius circle (r[s] = 0.73, $p < 0.001$, $n = 42$), (b) 100-km-radius circle (r[s] = 0.70, $p < 0.001$, $n = 42$), and (c) 600- × 200-km oval (r[s] = 0.70, $p < 0.001$, $n = 41$).

axis oriented northwest–southeast, approximately parallel to the California coast and centered on Sta. M (Fig. 1). Net primary production (NPP) was calculated from satellite chlorophyll, photosynthetically available radiation (PAR), and SST with the vertically generalized production model of Behrenfeld and Falkowski (1997). Export flux (EF) from the euphotic zone was estimated by combining NPP and SST via the parameterization of Laws (2004). These methods of time-series analysis within discrete geographic regions are described by Kahru and Mitchell (2000, 2002).

Spearman rank cross-correlations were calculated with the use of monthly averages with monthly time lags to evaluate the intensity and timing of relationships between climate indices, surface-water conditions, and POC flux to the seafloor (Zar 1998). *P* values were corrected for serial autocorrelation by the modified Chelton method (Pyper and Peterman 1998).

Results

POC flux, at 600 and 50 m above the bottom (mab), exhibited seasonal as well as interannual fluctuations from June 1989 through October 2004 (Fig. 2a). The declining trend in POC flux through 1996 was followed by a resurgence in food supply that began in 1998 and reached peaks in 2002 and 2003 comparable to those measured in the summers of 1991 and 1994. POC fluxes at 600 and 50 mab were compared during periods when measurements were available at both altitudes. These two monthly POC flux records were correlated highly and significantly (Spearman [s] $r = 0.86$, $p < 0.0001$, $n = 90$). The ratio of POC flux at 600 mab to flux at 50 mab generally was less than unity, except during periods in 1990/1991 and 1996 (Fig. 2b).

POC flux was compared with three climate indices. The MEI exhibited a major sustained peak in 1997/1998 during a strong ENSO event, whereas the NOI showed a large depression at about the same time (Fig. 2c). Annual peaks in BUI were evident throughout the measurement period, but the amplitude increased in 1999, suggesting strong upwelling in 1999 following the ENSO event in the previous year (Fig. 2d). A hiatus in POC flux measurements from 1999 to mid-2001 precludes a comparison with climate indices during this period of enhanced upwelling. However, when sampling was resumed in 2001, POC fluxes had increased above values measured over the previous 7 yr, with a large peak in the fall 2002 (Fig. 2a) following a high in BUI earlier in the same year (Fig. 2d).

Monthly averaged POC flux at both altitudes was compared with the MEI and NOI, climate indices that reflect

processes on a broad oceanic scale. POC flux lagged the MEI by 9 to 10 months, but the interpretation of the NOI comparison was not as distinct (Fig. 3a,b,d,e). Stronger correlations were observed in the POC flux comparisons from 50 mab, probably because of the more complete data set from this altitude. On a more regional scale, peaks in BUI occurred 2 to 3 months before peaks in POC fluxes at both altitudes (Fig. 3c,f), suggesting a close temporal connection between the upwelling of cold, nutrient-rich water and the arrival of sinking POC to the abyss. Satellite-derived SSTs were virtually identical for the three selected catchment areas surrounding Sta. M (Fig. 4a).

A missing step in this analysis of climate forcing and POC flux at abyssal depths is the production of organic carbon in surface waters. High-resolution satellite ocean color data are available only from November 1996 to the present, but these afford the best existing means for estimating primary production and EF from the euphotic zone. Chlorophyll *a* (Chl *a*) concentration was estimated from OCTS and SeaWiFS monthly data for the three catchment areas around Sta. M (Fig. 1). Monthly averaged Chl *a* concentrations for each of these three catchment areas were conspicuously low in 1998, corresponding to a major ENSO event, but were higher and relatively consistent from 1999 through early 2003, when fluctuations became greater in amplitude (Fig. 4b).

Chl *a* was similar among the three catchment areas for most of the time series but did show some discrepancies, with higher values in the large oval than the two smaller circles during several time periods from late 2001 until mid-2004 (Fig. 4b). NPP, calculated from satellite chlorophyll, PAR, and SST, closely tracked Chl *a* (Fig. 4c).

The portion of the NPP exported from the euphotic zone and contributing to the measured POC flux at abyssal depths was calculated as EF (Laws 2004). The EF model predicts higher EFs from the euphotic zone, with reduced microbial activity at lower temperatures, whereas EF is lower at higher temperatures with enhanced microbial activity. Comparisons between EF and POC flux to the seafloor are limited to the 50-mab record because of the limited data for the 600-mab trap after November 1996 when the EF data are available. The period of elevated EF in the second half of 1998 was associated with higher POC fluxes, primarily at 50 mab, and continued higher fluxes after the sampling hiatus during 2001 (Fig. 4d,e). Cross-correlations between EF and POC flux at 50 mab were calculated during periods when both data sets existed (Fig. 3g,h,i). Temporal lags between the two parameters ranged from <1 month for the 50-km-radius circle ($r[s] = 0.47$, $p < 0.01$, $n = 42$) to 3 months for the large oval ($r[s] = 0.54$, $p < 0.01$, $n = 41$).

Although the climate, surface-water, and abyssal data sets are not completely synoptic throughout the 15-yr time series at Sta. M, there are strong implications that climate change can be tracked from the surface ocean to the abyssal seafloor. An ENSO event in 1998 and upwelling events in 1999 and 2002 correlated with observed changes in POC flux at 600 mab and especially at 50 mab. Given the difficulty of making measurements in the deep ocean on broad spatial and temporal scales, it is tantalizing to propose that global climate and satellite data can be used to estimate basic deep-ocean biogeochemical processes.

An empirical model was created with the use of multiple regressions of POC flux data from November 1996 through October 2004 and records of EF, BUI, and NOI, with temporal lags on the basis of cross-correlation analysis (Fig. 3). A separate set of model parameters was created for each of the three catchment areas over Sta. M (Fig. 1) because each area had a different peak temporal lag, as determined by cross-correlation analysis (Fig. 3). The empirical tuning parameters (*a*, *b*, *c*, and the *y*-intercept) were evaluated with multiple regressions [estimated POC $\text{flux}_{50\ \text{mab}}$ = EF(*a*) + BUI(*b*) + NOI(*c*) + *y*-intercept]. Reasonable agreement exists between predicted and measured POC fluxes for all three catchment areas (Fig. 5; 50-km radius, $r[s] = 0.73$, $p < 0.001$, $n = 42$; 100-km radius, $r[s] = 0.70$, $p < 0.001$, $n = 42$; oval, $r[s] = 0.70$, $p < 0.001$, $n = 41$). Discrepancies between the measured and predicted fluxes were evident between August 2001 and May 2002 and between October 2003 through 2004 for all three spatial configurations (Fig. 5). Although these discrepancies are noteworthy, the greatest departures are roughly 50% of the overall variability in the model.

Discussion

There was a strong correlation between POC flux measured at both 600 and 50 mab (3,500- and 4,050-m depth) at Sta. M and climate indices lagged by various intervals. The basin-scale indices MEI and NOI were correlated with POC flux at longer time intervals of 6 to 10 months, whereas the regional BUI was correlated with POC flux at a lag of only 2 to 3 months (Fig. 3). It seems reasonable that elevated upwelling intensity, cold surface waters, and high EF would be correlated significantly with high POC flux at Sta. M. EF from the euphotic zone was estimated from satellite color and SST. EF was positively correlated with POC flux with the use of three different spatial configurations for surface catchment areas: circles with radii of 50 and 100 km and a much larger oval measuring 600 × 200 km. The time lag between records of EF and POC flux increased with increasing size of the catchment area: no lag for the 50-km circle to 3 months for the large oval. A model to estimate POC flux at Sta. M with NOI, BUI, and satellite-derived EF data yielded significant agreement to observed fluxes over the period when satellite data overlapped with our most extensive POC flux records from 50 mab. POC flux data from 600 mab were insufficient to conduct a similar analysis. However, it is interesting to note that even with evidence of lateral advection in the deeper sediment trap (50 mab, Fig 2b), there still was a significant correlation between climate indices and surface-water parameters. Lateral advection at 50 mab has been estimated to range from 1.5% to 20.9% of the annual POC flux at Sta. M (Smith et al. 2001), with the most probable source being the continental shelf and slope to the northeast (Bianchi et al. 1998; Druffel et al. 1998). Larger scale influences of climate and surface-water conditions probably influence lateral advection, as well as the fluxes of pelagically derived particulate matter at Sta. M. Unresolved temporal variability in pelagic community dynamics and subsequent particulate matter sinking rates

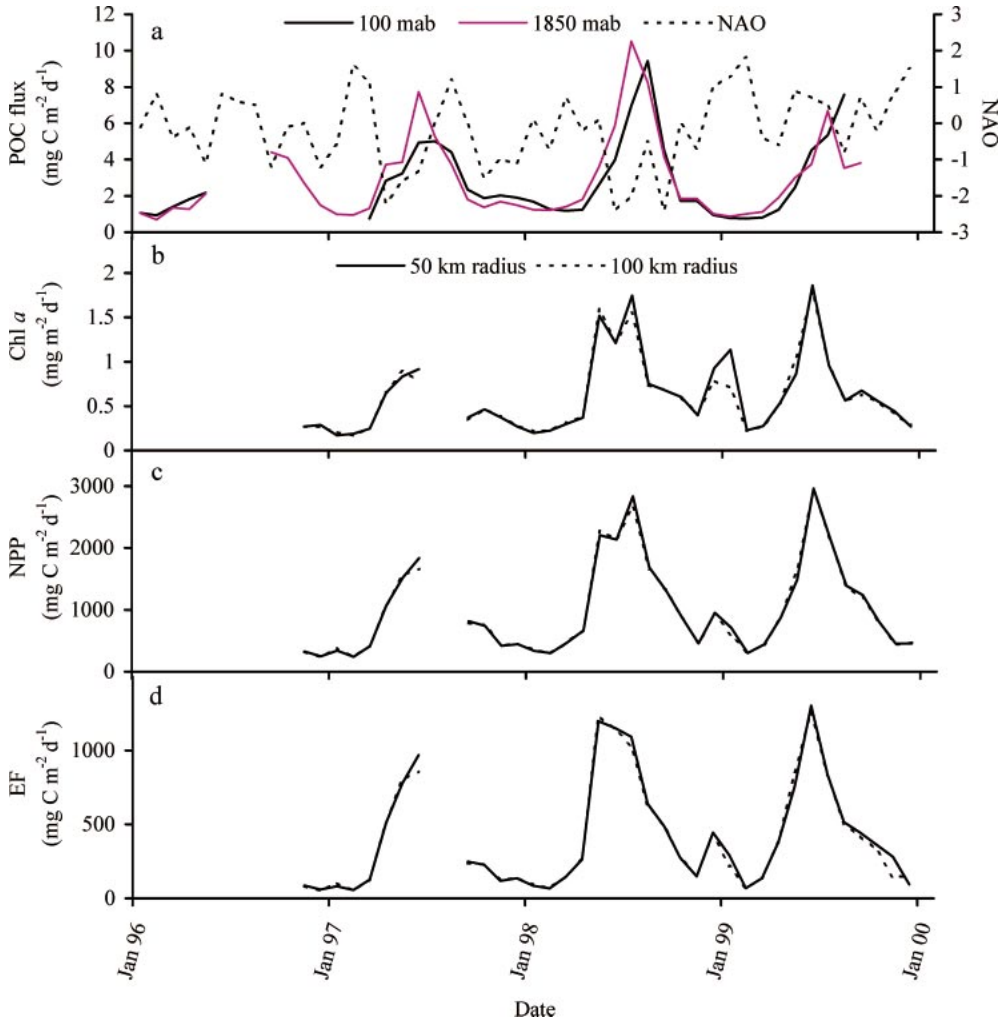

Fig. 6. Time-series comparison of monthly averaged POC flux at 1,850 and 100 mab at Sta. PAP in the northeast Atlantic, with the monthly NAO climate index, estimated surface Chl *a*, net primary production (NPP), and export flux (EF). (a) NAO index and POC flux at 1,850 and 100 mab, (b) Chl *a* for 50- and 100-km-radius circles above Sta. PAP, (c) NPP for 50- and 100-km-radius circles, and (d) EF for 50- and 100-km-radius circles.

might also contribute to differences between model estimated and measured fluxes at abyssal depths.

A connection between planktonic production and EF to the deep ocean as particulate organic matter first was evaluated by Eppley and Peterson (1979). Since this initial report, additional evidence has been collected to support the connection between surface processes and the supply of organic matter to the deep ocean. Oxygen isotopic signatures of epipelagic foraminifera collected in a sediment trap at 3,200-m depth, 1,000 m above the seafloor in the northwest Atlantic, were correlated to surface-water hydrographic events with a time lag of 1 month (Deuser 1986). Ocean color events, identified with the Coastal Zone Color Scanner (Deuser 1986), were found to correspond with sinking POC flux measured over a 7-yr period at the same site and depth (Deuser et al. 1990). Changes in ocean color and the flux of POC at this site in the northwest Atlantic were correlated with a 1.5-month lag, a similar period to our results from the northeast Pacific. The spatial origin of the particulate matter collected in the deep northwest Atlantic was termed the ''statistical funnel.'' The size of this funnel was calculated with a Lagrangian analysis based on the velocity field above the trap, collection period, and estimated sinking speeds of particles (Siegel and Deuser 1997). Their analysis showed that sinking particles approach horizontal trajectories, resulting in a large statistical funnel. The radius of the statistical funnel at the sea surface was ≥600 km for a sediment trap moored at 3,200 m in the northwest Atlantic (Siegel and Armstrong 2002). Even with the complexity of the hydrographic conditions off the central California margin in the area overlying Sta. M, the smallest statistical funnel examined in our study (50-km-radius circle) provided the shortest lag between EF and POC flux at 4,050-m depth. In dynamic hydrographic conditions such as those present off central California, a smaller statistical funnel might be more realistic than a larger one for exhibiting variability in surface characteristics of comparable magnitude and with similar timescales to measurements (e.g. POC flux) made directly below.

To examine the general value of our approach in studying

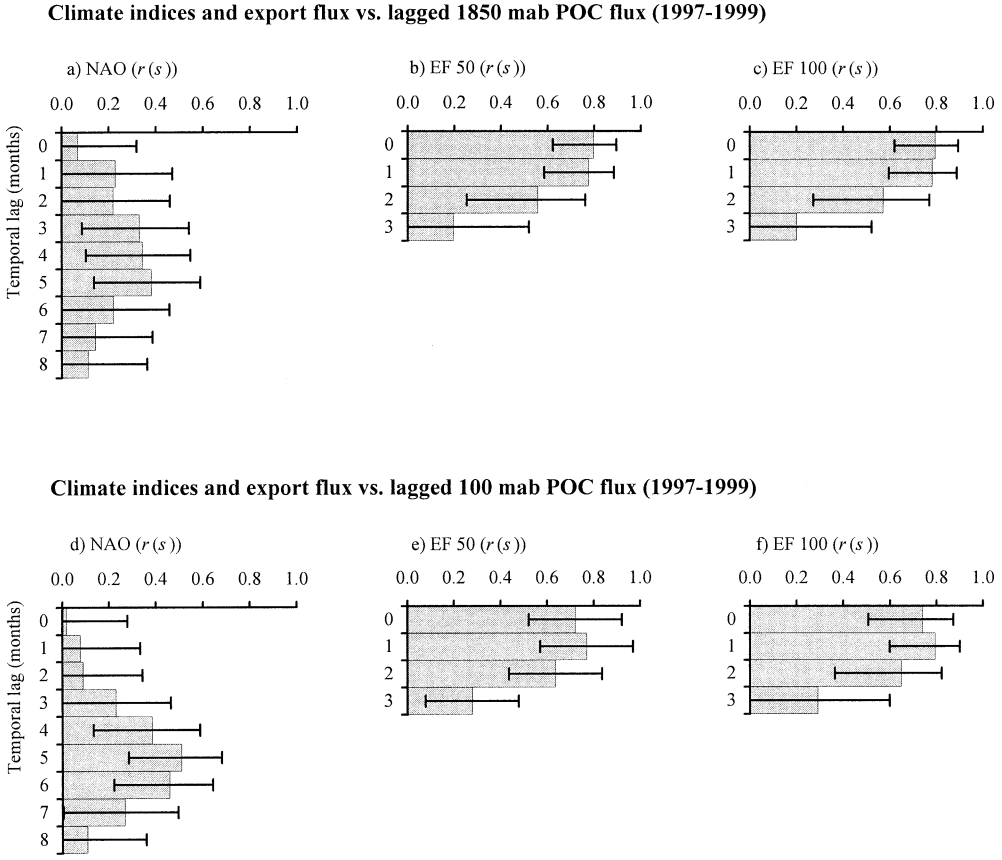

Fig. 7. Cross-correlation analysis of NAO index and export flux (EF) computed for 50-and 100-km-radius circles over Sta. PAP when lagged monthly to measured POC flux at 1,850 and 100 mab. (a) NAO lagged to POC flux at 100 mab. (b) EF computed for 50-km-radius circle lagged to POC flux at 100 mab. (c) EF computed for 100-km-radius circle lagged to POC flux at 100 mab. (d) NAO lagged to POC flux at 1,850 mab. (e) EF computed for 50-km-radius circle lagged to POC flux at 1,850 mab. (f) EF computed for 100-km-radius circle lagged to POC flux at 1,850 mab. Error bars represent 95% confidence intervals for each month.

the relationship among climate indicators, satellite ocean color, and POC flux to the deep ocean, we also examined data gathered from a long time-series abyssal station in the northeast Atlantic on the Porcupine Abyssal Plain (Sta. PAP, 4,850-m depth; Lampitt et al. 2001). At this site, POC flux was measured at 3,000- and 4,750-m depth, 1,850 and 100 mab, respectively, from 1989 through 2000, with a long hiatus covering most of the period between 1991 and late 1996. Between January 1997 and late 1999, the POC flux had one high peak at both depths during the summer of 1998 and another maximum in spring/summer 1999 (Fig. 6a). The North Atlantic Oscillation (NAO), a basin-scale monthly climate index based on the sea level pressure difference between the subtropical and subpolar North Atlantic (http://www.cpc.ncep.noaa.gov/data/teledoc/nao.html), was correlated significantly with POC flux at 1,850 mab (r[s] = 0.33, $p \leq$ **0.019,** n = 63) and 100 mab (r[s] = 0.51, $p < 0.001$, n = 56) at Sta. PAP when lagged by 5 months (Fig. 7a,d). A positive NAO index is associated with strong winter storm conditions in the North Atlantic (Visbeck et al. 1998). As previously described for Sta. M, surface ocean Chl *a* was estimated from satellite ocean color data for 50- and 100-km-radius circles around Sta. PAP, beginning in 1997 and extending through 1999 (Fig. 6b). NPP exhibited annual peaks of increasing magnitude from 1997 through 1999 (Fig. 6c), and EF showed a similar trend (Fig. 6d). EF was correlated positively with POC flux at 1,850 and 100 mab; highest correlations were observed at lags of 0–1 month for both the 50-km and 100-km-radius circles over Sta. PAP (Fig. 7b,c,e,f). A similar lag period between EF and POC flux was found at Sta. M, especially for the 50-km-radius circle, suggesting that the average sinking rate of particulate matter to abyssal depths is similar at the northeast Pacific and northeast Atlantic locations. The smallest catchment area (50-km-radius circle) provided the shortest lag between EF and POC flux at Sta. M, whereas larger areas increased the lag period (Fig. 3g–i). In contrast, lag period did not change appreciably between EF and POC flux at Sta. PAP with increased catchment area (Fig. 7e,f). Higher complexity of hydrographic conditions surrounding Sta. M are probably a contributing factor to this difference between the northeast Pacific and northeast Atlantic stations.

A similar modeling effort with an upper ocean biogeochemistry model was applied to the Sta. PAP particle flux

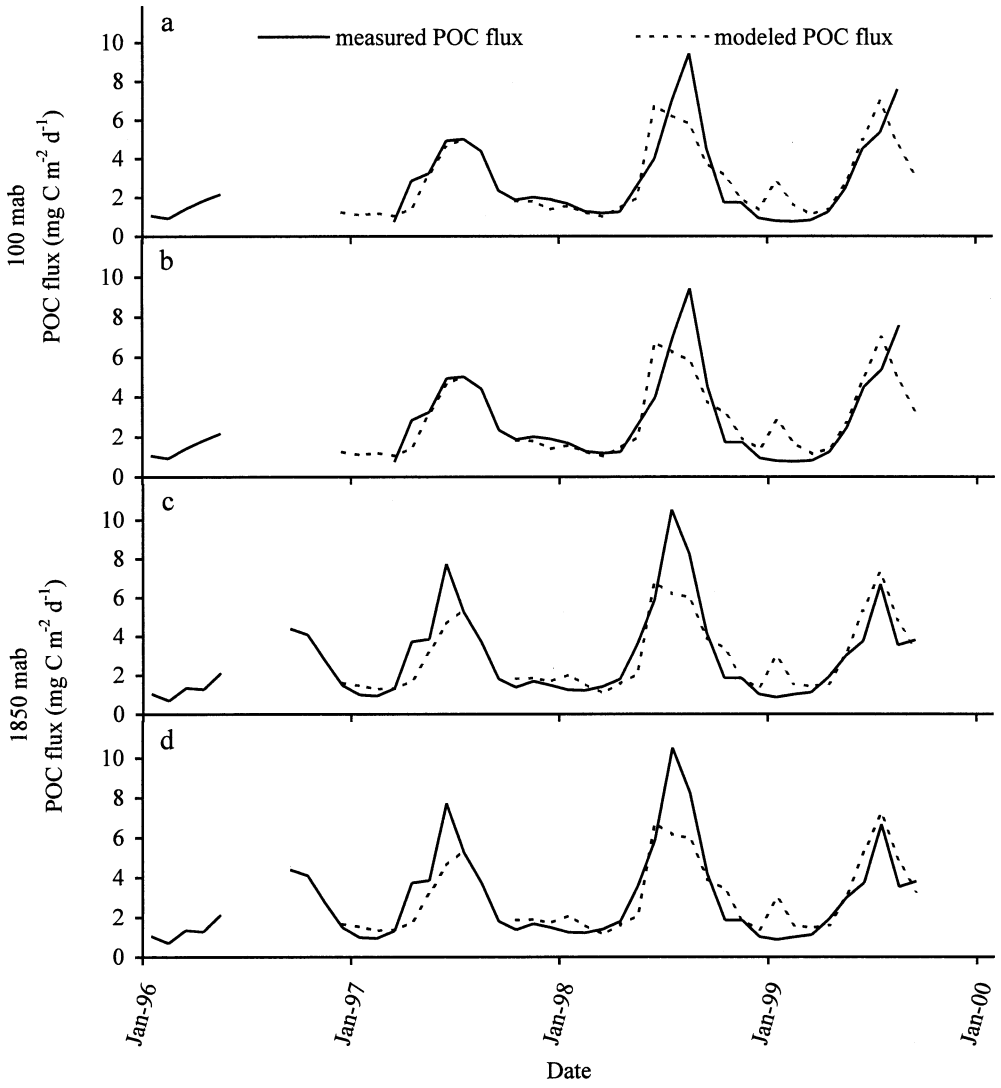

Fig. 8. Empirical model results for POC flux at 1,850 and 100 mab with the use of temporally lagged NAO and export flux for a 50- and 100-km-radius catchment circle over Sta. PAP. (a) POC flux at 100 mab with 50-km-radius catchment circle (r[s] = 0.82, $p < 0.0001$, $n = 28$). (b) POC flux at 100 mab with 100-km-radius catchment circle (r[s] = 0.82, $p < 0.001$, $n = 28$). (c) POC flux at 1,850 mab with 50-km-radius catchment circle (r[s] = 0.80, $p < 0.001$, $n = 33$). (d) POC flux at 1,850 mab with 100-km-radius catchment circle (r[s] = 0.79, $p < 0.001$, $n = 33$).

results from 1,850 mab (3,000-m depth) to avoid resuspension events noted in the 100-mab collections (Lampitt et al. 2001). They reported good agreement between the predicted and measured POC flux on an annual basis, but no significant relationship was apparent on interannual timescales.

We developed a model to estimate POC flux for both the 1,850- and 100-mab sediment traps at Sta. PAP with EF and NAO data. An upwelling index was not used because wind–upwelling relationships in the northeast Atlantic are less consistent than along the west coast of North America, where bathymetry and coastal topography create a strong upwelling system. Only 50- and 100-km catchment areas over Sta. PAP were applied to examine EF relationships with POC flux; the larger oval was tailored for the North American coastline and would not have been appropriate for Sta. PAP. Our model estimated the measured POC flux at Sta. PAP at both spatial configurations with reasonable success, with the exception of the summer of 1998 at both depths and the summer of 1997 at 1,850 mab, when predicted values were notably lower (Fig. 8). Significant correlations were found between predicted and measured POC fluxes at both 1,850 mab (50-km radius, r[s] = 0.80, $p < 0.0001$, $n = 33$; 100-km radius, r[s] = 0.79, $p < 0.0001$, $n = 33$; Fig. 8c,d) and 100 mab (50-km radius, r[s] = 0.82, $p < 0.001$, $n = 28$; 100-km radius, r[s] = 0.82, $p < 0.0001$, $n = 28$; Fig. 8a,b). At the spatial and temporal scales used in our modeling, the difference between the 1,850- and 100-mab POC fluxes was minimal.

The results from Sta. M in the abyssal northeast Pacific and from Sta. PAP in the abyssal northeast Atlantic suggest a strong relationship between EF generated from satellite imagery according to the Laws (2004) model and POC flux-

es measured at abyssal depths. The empirical models proposed here were created for specific locations. Nonetheless, the relationships described by these models indicate that estimating deep-sea processes with climate indices and satellite sensing does appear feasible over broad areas.

References

BAKUN, A. 1973. Coastal upwelling indices, west coast of North America, 1946–1971. NOAA Technical Report NMFS SSRF-671.

BALDWIN, R. J., R. C. GLATTS, AND K. L. SMITH, JR. 1998. Particulate matter fluxes into the benthic boundary layer at a long time-series station in the abyssal NE Pacific: Composition and fluxes. Deep-Sea Res. II **45:** 643–666.

BEAULIEU, S., AND R. BALDWIN. 1998. Temporal variability in currents and the benthic boundary layer at an abyssal station off central California. Deep-Sea Res. II **45:** 587–615.

BEHRENFELD, M. J., AND P. G. FALKOWSKI. 1997. Photosynthetic rates derived from satellite-based chlorophyll concentration. Limnol. Oceanogr. **42:** 1–20.

BIANCHI, T. S., J. E. BAUER, E. R. M. DRUFFEL, AND C. D. LAMBERT. 1998. Pyrophaeophorbide-*a* as a tracer of suspended particulate organic matter from the NE Pacific continental margin. Deep-Sea Res. II **45:** 715–731.

BILLETT, D. S. M., B. J. BETT, A. L. RICE, M. H. THURSTON, J. GALERON, M. SIBUET, AND G. A. WOLFF. 2001. Long-term changes in the megabenthos of the Porcupine Abyssal Plain (NE Atlantic). Prog. Oceanogr. **50:** 325–348.

BOGRAD, S. J., P. M. DIGIACOMO, R. DURAZO, AND OTHERS. 2000. The state of the California Current, 1999–2000: Forward to a new regime? CalCOFI Rep. **41:** 26–52.

CHAVEZ, F. P., J. RYAN, S. E. LLUCH-COTA, AND M. C. NIQUEN. 2003. From anchovies to sardines and back: Multidecadal change in the Pacific Ocean. Science **299:** 217–221.

DEUSER, W. G. 1986. Seasonal and interannual variations in deep-water particle fluxes in the Sargasso Sea and their relation to surface hydrography. Deep-Sea Res. **33:** 225–246.

———, F. E. MULLER-KARGER, R. H. EVANS, O. B. BROWN, W. E. ESAIAS, AND G. C. FELDMAN. 1990. Surface-ocean color and deep-ocean carbon flux: How close a connection? Deep-Sea Res. **37:** 1331–1343.

———, AND E. H. ROSS. 1980. Seasonal change in the flux of organic carbon to the deep Sargasso Sea. Nature **283:** 364–365.

DRUFFEL. E. R. M., S. GRIFFIN, J. E. BAUER, D. M. WOLGAST, AND X.-C. WANG. 1998. Distribution of particulate organic carbon and radiocarbon in the water column from the upper slope to the abyssal NE Pacific Ocean. Deep-Sea Res. II **45:** 667–687.

EPPLEY, R. W., AND B. J. PETERSON. 1979. Particulate organic matter flux and planktonic new production in the deep ocean. Nature **282:** 677–680.

KAHRU, M., AND B. G. MITCHELL. 2000. Influence of the 1997–98 El Nino on the surface chlorophyll in the California Current. Geophys. Res. Lett. **27:** 2937–2940.

———, AND ———. 2001. Seasonal and nonseasonal variability of satellite-derived chlorophyll and colored dissolved organic matter concentration in the California Current. J. Geophys. Res. **106:** 2517–2529.

———, AND ———. 2002. Influence of the El Nino–La Nina cycle on satellite-derived primary production in the California Current. Geophys. Res. Lett. **29:** 1846.

LAMPITT, R. S., B. J. BETT, K. KIRIAKOULAKIS, E. E. POPOVA, O. RAGUENEAU, A. VANGRIESHEIM, AND G. A. WOLFF. 2001. Material supply to the abyssal seafloor in the Northeast Atlantic. Prog. Oceanogr. **50:** 27–63.

LAWS, E. A. 2004. Export flux and stability as regulators of community composition in pelagic marine biological communities: Implications for regime shifts. Prog. Oceanogr. **60:** 343–354.

MCGOWAN, J. A., S. J. BOGRAD, R. J. LYNN, AND A. J. MILLER. 2003. The biological response to the 1977 regime shift in the California Current. Deep-Sea Res. II **50:** 2567–2582.

MITCHELL, B. G., AND M. KAHRU. 1998. Algorithms for SeaWiFS standard products developed with the CalCOFI bio-optical data set. Calif. Coop. Ocean. Fish. Invest. Rep. **39:** 133–147.

O'REILLY, J. E., S. MARITORENA, B. G. MITCHELL, AND OTHERS. 1998. Ocean color chlorophyll algorithms for SeaWiFS. J. Geophys. Res. **103:** 24,937–24,953.

PYPER, B. J., AND R. M. PETERMAN. 1998. Comparison of methods to account for autocorrelation in correlation analyses of fish data. Can. J. Fish. Aquat. Sci. **55:** 2127–2140.

ROEMMICH, D., AND J. MCGOWAN. 1995. Climatic warming and the decline of zooplankton in the California Current. Science **267:** 1324–1326.

RUHL, H. A., AND K. L. SMITH, JR. 2004. Shifts in deep-sea community structure linked to climate and food supply. Science **305:** 513–515.

SAGARIN, R. D., J. P. BARRY, S. E. GILMAN, AND C. H. BAXTER. 1999. Climate-related changes in an intertidal community over short and long time scales. Ecol. Monogr. **69:** 465–490.

SCHWING, F. B., T. MURPHREE, AND P. M. GREEN. 2002. The Northern Oscillation Index (NOI): A new climate index for the northeast Pacific. Prog. Oceanogr. **53:** 115–139.

SIEGEL, D. A., AND R. A. ARMSTRONG. 2002. Corrigendum to ''Trajectories of sinking particles in the Sargasso Sea: Modeling of statistical funnels above deep-ocean sediment traps'' [Deep-Sea Research I 44, 1519–1541]. Deep-Sea Res. I **49:** 1115–1116.

———, AND W. G. DEUSER. 1997. Trajectories of sinking particles in the Sargasso Sea: Modeling of statistical funnels above deep ocean sediment traps. Deep-Sea Res. I **44:** 1519–1541.

SMITH, K. L., JR., AND R. J. BALDWIN. 1984. Seasonal fluctuations in deep-sea sediment community oxygen consumption: Central and eastern North Pacific. Nature **307:** 624–625.

———, ———, R. C. GLATTS, AND R. S. KAUFMANN. 1998. Detrital aggregates on the sea floor: Chemical composition and aerobic decomposition rates at a time-series station in the abyssal NE Pacific. Deep-Sea Res. II **45:** 843–880.

———, AND E. R. M. DRUFFEL. 1998. Long time-series studies of the benthic boundary layer at an abyssal station in the NE Pacific. Deep-Sea Res. II **45:** 573–586.

———, AND R. S. KAUFMANN. 1999. Long-term discrepancy between food supply and demand in the deep eastern North Pacific. Science **284:** 1174–1177.

———, ———, R. J. BALDWIN, AND A. F. CARLUCCI. 2001. Pelagic–benthic coupling in the abyssal eastern North Pacific: An eight-year time-series study of food supply and demand. Limnol. Oceanogr. **46:** 543–556.

VISBECK, M., H. CULLEN, G. KRAHMANN, AND N. NAIK. 1998. An ocean model's response to North Atlantic Oscillation–like wind forcing. Geophys. Res. Lett. **25:** 4521–4524.

WOLTER, K., AND M. S. TIMLIN. 1998. Measuring the strength of ENSO events: How does 1997/98 rank? Weather **53:** 315–324.

ZAR, J. H. 1998. Biostatistical analysis, 4th ed. Prentice Hall.

Received: 23 June 2004
Accepted: 16 July 2005
Amended: 28 July 2005